

UCSF

UC San Francisco Previously Published Works

Title

Cooperative loss of RAS feedback regulation drives myeloid leukemogenesis

Permalink

<https://escholarship.org/uc/item/5jw5d1tb>

Journal

Nature Genetics, 47(5)

ISSN

1061-4036

Authors

Zhao, Zhen

Chen, Chi-Chao

Rillahan, Cory D

et al.

Publication Date

2015-05-01

DOI

10.1038/ng.3251

Peer reviewed



Published in final edited form as:

Nat Genet. 2015 May ; 47(5): 539–543. doi:10.1038/ng.3251.

Cooperative loss of RAS feedback regulation drives myeloid leukemogenesis

Zhen Zhao¹, Chi-Chao Chen^{1,2}, Cory D. Rillahan¹, Ronglai Shen³, Thomas Kitzing¹, Megan E. McNerney⁴, Ernesto Diaz-Flores⁵, Johannes Zuber⁶, Kevin Shannon⁵, Michelle M. Le Beau⁷, Mona S. Spector⁸, Scott C. Kogan⁹, and Scott W. Lowe^{1,10}

¹Cancer Biology and Genetics Program, Memorial Sloan-Kettering Cancer Center, New York, NY, USA

²Weill Cornell Graduate School of Medical Sciences, Cornell University, New York, NY, USA

³Department of Epidemiology & Biostatistics, Memorial Sloan-Kettering Cancer Center, New York, NY, USA

⁴Department of Pathology, Department of Pediatrics, Section of Hematology/Oncology, University of Chicago, Chicago, IL, USA

⁵Department of Pediatrics, University of California, San Francisco, CA, USA

⁶Research Institute of Molecular Pathology (IMP), Vienna Biocenter (VBC), Vienna, Austria

⁷Section of Hematology/Oncology, Department of Medicine, University of Chicago, Chicago, IL, USA

Users may view, print, copy, and download text and data-mine the content in such documents, for the purposes of academic research, subject always to the full Conditions of use:http://www.nature.com/authors/editorial_policies/license.html#terms

To whom correspondence should be addressed: Scott W. Lowe, Memorial Sloan-Kettering Cancer Center, 415 E. 68th Street, Z-1114, New York, NY 10065, lowes@mskcc.org.

URLs

cBioPortal link

[http://www.cbioportal.org/public-portal/index.do?](http://www.cbioportal.org/public-portal/index.do?cancer_study_id=laml_tcga&genetic_profile_ids_PROFILE_MUTATION_EXTENDED=laml_tcga_mutations&genetic_profile_ids_PROFILE_COPY_NUMBER_ALTERATION=laml_tcga_gistic&Z_SCORE_THRESHOLD=2.0&data_priority=0&case_set_id=laml_tcga_cnaseq&case_ids=&gene_set_choice=user-defined-list&gene_list=FLT3%3AGAIN%2CAMP%2CMUT%3B%0D%0AKIT%3AGAIN%2CAMP%2CMUT%3B%0D%0AKRAS%3AGAIN%2CAMP%2CMU%3B%0D%0ANRAS%3AGAIN%2CAMP%2CMUT%3B%0D%0ATP53%3AAMP%2CMUT%2CHOMDEL%2C+HETLOSS%3B%0D%0ANF1%3AMUT%2CHOMDEL%2C+HETLOSS%3B%0D%0ADUSP14%3AMUT%2CHOMDEL%2C+HETLOSS%3B%0D%0ARASA1%3AMUT%2CHOMDEL%2C+HETLOSS%3B%0D%0ASPRY4%3AMUT%2CHOMDEL%2C+HETLOSS%3B%0D%0ADUSP1%3AMUT%2CHOMDEL%2C+HETLOSS%3B&clinical_param_selection=null&tab_index=tab_visualize&Action=Submit)

http://www.cbioportal.org/public-portal/index.do?cancer_study_id=laml_tcga&genetic_profile_ids_PROFILE_MUTATION_EXTENDED=laml_tcga_mutations&genetic_profile_ids_PROFILE_COPY_NUMBER_ALTERATION=laml_tcga_gistic&Z_SCORE_THRESHOLD=2.0&data_priority=0&case_set_id=laml_tcga_cnaseq&case_ids=&gene_set_choice=user-defined-list&gene_list=FLT3%3AGAIN%2CAMP%2CMUT%3B%0D%0AKIT%3AGAIN%2CAMP%2CMUT%3B%0D%0AKRAS%3AGAIN%2CAMP%2CMU%3B%0D%0ANRAS%3AGAIN%2CAMP%2CMUT%3B%0D%0ATP53%3AAMP%2CMUT%2CHOMDEL%2C+HETLOSS%3B%0D%0ANF1%3AMUT%2CHOMDEL%2C+HETLOSS%3B%0D%0ADUSP14%3AMUT%2CHOMDEL%2C+HETLOSS%3B%0D%0ARASA1%3AMUT%2CHOMDEL%2C+HETLOSS%3B%0D%0ASPRY4%3AMUT%2CHOMDEL%2C+HETLOSS%3B%0D%0ADUSP1%3AMUT%2CHOMDEL%2C+HETLOSS%3B&clinical_param_selection=null&tab_index=tab_visualize&Action=Submit

TCGA data portal

<https://tcga-data.nci.nih.gov/tcga/tcgaCancerDetails.jsp?diseaseType=LAML&diseaseName=Acute%20Myeloid%20Leukemia>.

Jackson Laboratory

<http://www.jax.org/index.html>

Author Contributions

Z.Z. designed, performed and analyzed the experiments. C.C. cloned miRE shRNA and performed Gene Set Enrichment Analysis. C.C. and R.S. analyzed expression pattern of TCGA data and performed statistical analysis for all bioinformatics results. M.E.M. and M.M.L. provided 35 patients RNA seq, SNParray and partial karyotyping data from UCM. T.K. analyzed the cBioPortal database. *In vivo* phospho-FACS experiments were performed by Z.Z. and E.D.F. with suggestions from K.M.S. J.Z. cloned sh*Spry4* related constructs and suggested *in vivo* experiments. M.S.S. initially analyzed deletion and mutational data of *SPRY4* and suggested experiments. S.C.K. characterized the phenotype and immunophenotype of models and helped to design experiments. S.W.L. designed and analyzed experiments, and supervised the work. Z.Z., C.D.R., and S.W.L. wrote the paper and M.S.S. revised the manuscript.

⁸Cold Spring Harbor Laboratory, Cold Spring Harbor, NY, USA

⁹Department of Laboratory Medicine & Helen Diller Family Comprehensive Cancer Center, University of California San Francisco, San Francisco, CA, USA

¹⁰Howard Hughes Medical Institute, New York, NY, USA

Abstract

RAS network activation is common in human cancers and, in acute myeloid leukemia (AML), achieved mainly through gain-of-function mutations in *KRAS*, *NRAS*, or the *FLT3* receptor tyrosine kinase¹. In mice, we show that premalignant myeloid cells harboring a *Kras*^{G12D} allele retain low Ras signaling owing to a negative feedback involving *Spry4* that prevents transformation. In humans, *SPRY4* is located on chromosome 5q, a region affected by large heterozygous deletion that are associated with an aggressive disease in which gain-of-function RAS pathway mutations are rare. These 5q deletions often co-occur with chromosome 17 alterations involving deletion of *NF1* - another RAS negative regulator - and *TP53*. Accordingly, combined suppression of *Spry4*, *Nf1* and *Trp53* produces high Ras signaling and drives AML in mice. Therefore, *SPRY4* is a 5q tumor suppressor whose disruption contributes to a lethal AML subtype that appears to acquire RAS pathway activation through loss of negative regulators.

Acute myeloid leukemia (AML) is a heterogeneous cancer that represents the most common form of acute leukemia in adults². Cytogenetic and molecular profiling of human AML samples has identified a range of missense mutations, translocations, and large chromosomal events that can be associated with different patient outcomes^{1,3}. Among the most common genetic events in AML involve gain-of-function mutations in the RAS pathway, including activating mutations of *KRAS* and *NRAS* genes themselves or upstream receptor tyrosine kinases *FLT3* or *KIT*^{1,3}. Each of these mutations produce altered proteins that directly or indirectly drive RAS GTPase into a constitutively active GTP bound state⁴, and lead to leads to constitutive activation of the mitogen activated protein kinase (MAPK) and phosphoinositide-3-kinase (PI3K) pathways⁴. While these lesions are considered important drivers of disease, *RAS* mutations alone are often unable to produce the high levels of MAPK and PI3K signaling necessary for malignant transformation without corresponding increases in mutant *KRAS* or *NRAS* copy number or other mechanisms that increase RAS output^{5,6,7}.

Previously we found that *Kras*^{G12D} activation cooperates with RNAi-mediated *Trp53* inactivation to induce AML in mice⁸, and these AMLs had markedly elevated levels of pERK (a MAPK effector) and pS6 (an effector of both MAPK and PI3K) in both primary leukemia and transplanted secondary AML, even in the absence of cytokine GM-CSF stimulation (Fig. 1a, 1b)⁸. However, consistent with previous work^{5,6,9,10}, *Kras*^{G12D} alone was unable to trigger a basal or cytokine-induced increase in pERK or pS6 levels in bulk bone marrow cells, Kit⁺ progenitors, or Mac-1⁺ mature myeloid cells as assessed by flow cytometry (Fig. 1a, 1b, Supplementary Fig. 1a-d). Thus, while highly activated Ras signaling appears to be an intrinsic feature of these AMLs, endogenous expression of oncogenic *Kras*^{G12D} is insufficient to sustain constitutive activation of downstream effectors in non-transformed myeloid cells. While in some systems high pErk levels can be achieved

via somatic duplication or amplification of the *Kras*^{G12D} allele^{5,6}, these events cannot explain the strong pathway activation occurring in our AML model as no increase in *Kras*^{G12D} allele balance⁸ or protein levels was observed (Supplementary Fig. 1e).

It is well-established that Ras activation can trigger compensatory feedback mechanisms that dampen signaling output^{11,12,13}. To test whether such mechanisms might modulate Ras signaling during leukemogenesis, we generated wildtype (WT) or *Kras*^{G12D}-expressing hematopoietic stem and progenitor cells (HSPCs) by transducing WT or *LSL-KRas*^{G12D} fetal liver cells with a GFP-coupled, self-deleting CreER (LGmCreER)⁸. After addition of tamoxifen to induce Cre activity and thereby activate the *Kras*^{G12D} allele⁸, we quantified the expression of ten known negative feedback genes¹¹ in GFP⁺ cells expressing myeloid markers (Supplementary Fig. 1f). Quantitative RT-PCR analysis revealed that *Spry4* was significantly up-regulated by mutant *Kras* expression (Fig. 1c) but under-expressed in *Kras*^{G12D};*shp53* leukemia compared to normal bone marrow (Fig. 1d).

The inverse correlation between *Spry4* expression and Ras effector pathway activation was particularly interesting given the role of Sprouty proteins as negative regulators of Ras/ MAPK signaling during development¹⁴. To test whether a *Spry4*-mediated feedback limits Ras induced leukemogenesis, we used the established transplantation-based approach to assess the impact of *Spry4* suppression on *Kras*^{G12D}-induced leukemogenesis^{8,15}. In this approach, control and *Spry4* shRNAs (Supplementary Fig. 2a, 2b) were transduced into *LSL-KRas*^{G12D} HSPCs using the LGmCreER vector and the resulting cells were treated with tamoxifen to activate *Kras*^{G12D}. Mice receiving HSPCs transduced with each of three *Spry4* shRNAs displayed accelerated onset of T-cell lymphoma driven by oncogenic *Kras*^{16,17} (Supplementary Fig. 2b). Thus, *Spry4* suppression cooperates with *Kras*^{G12D} during tumorigenesis.

To assess whether *Spry4* can also limit the development of myeloid leukemia, we biased the system against lymphoid disease by using C57BL/6J mice devoid of thymi (*Foxn1*^{nu}) as recipients. In these studies, we transduced two of the *Spry4* shRNAs validated above into *LSL-Kras*^{G12D};*Trp53*^{+/-} HSPCs, anticipating loss of the wild-type *Trp53* allele during leukemogenesis. Again, both *Spry4* shRNAs accelerated disease onset (Fig. 2a) (112 and 215 median survival for recipients of *Kras*^{G12D};*Trp53*^{+/-};*shSpry4* (KP-S) and *Kras*^{G12D};*Trp53*^{+/-};*shCtrl* (KP-C) HSPCs, respectively $p < 0.01$). Interestingly, *Trp53* remained intact in both KP-S and KP-C leukemias, suggesting p53 can function as a haploinsufficient tumor suppressor in this model (Supplementary Fig. 2c). Histopathological analyses of moribund animals revealed all KP-S and KP-C recipient mice developed histiocytic sarcomas, an aggressive tumor of monocyte-derived cells that manifests in spleen and liver (Fig. 2b, Supplementary Fig. 3a). Flow cytometry indicated that the spleens from KP-S recipients were massively enriched for cells expressing intermediate levels of the myeloid marker Mac-1 (Fig. 2c), and that these cells showed elevated levels of both pErk and pS6, which was exacerbated by serum stimulation (Fig. 2c). Importantly, the leukemic cells isolated from two independent KP-S mice induced secondary disease in sub-lethally irradiated recipient mice at 100% penetrance (Supplementary Fig. 3b). These results demonstrate that *Spry4* knockdown accelerates leukemia onset and potentiates *Kras*-mediated myeloid transformation by increasing Ras signaling output.

In humans, *SPRY4* is located at chromosome 5q31.3 and is frequently deleted in the context of del(5q) in patients with myelodysplastic syndrome (MDS), complex karyotype AML (CK-AML), and therapy-related myeloid neoplasms (t-MN)^{18,19,20}. Analysis of data from The Cancer Genome Atlas (TCGA)^{1,21,22} revealed that *SPRY4* is deleted in 17 out of 187 AML patients (9% overall deletion rate), as part of chromosome 5q (Fig. 3a top). These findings were confirmed in a separate cohort of 35 AML/t-MN. Here, *SPRY4* deletion, defined by SNP array analysis, was found in 12 of 13 samples with karyotyping-confirmed 5q abnormalities, as well as in one other sample with unknown cytogenetic information (Fig. 3a bottom). These observations, together with our functional studies, suggest a role for *SPRY4* in human leukemia.

Although oncogenic *Kras* and *Spry4* suppression can cooperate during tumorigenesis, *KRAS* and *NRAS* mutations are rarely observed in human del(5q) AML^{23,24}. Indeed, while 42% of human AMLs have gain-of-function RAS pathway mutations (*KRAS*, *NRAS*, *FLT3*, *KIT*), such mutations were significantly underrepresented in del(5q) AML harboring *SPRY4* deletion (only 3 out of the 17, Fisher's exact test $p = 0.025$). Instead, *SPRY4* deletion/del(5q) often co-occurs with *TP53* mutations and/or deletion of its locus on chromosome 17p (Fig. 3b, Supplementary Fig. 4, Supplementary Fig. 5a, 5b, $p < 0.0005$). In addition to *SPRY4*, del(5q) AML frequently harbors losses of other negative RAS regulators including *RASA1* (p120-RasGAP, 5q), *DUSP1* (5q), *DUSP14* (17q), and *NF1* (17q) (Fig. 3b, Supplementary Fig. 4, and Supplementary Fig. 5. Odds Ratio > 10 , $p < 0.0005$ for all combinations by cBioPortal, see cBioPortal link). Interestingly, analysis of transcriptional profiles revealed a significant overlap between gene ontology categories enriched in *SPRY4*/5q deletion AML and *NRAS* mutant AMLs (6 overlapping pathways; 5 down-regulated and 1 up-regulated; p -value = 1.7×10^{-5}) (Supplementary Fig. 6a). In addition, these *SPRY4*/5q AMLs displayed a gene-set enrichment signature and a global gene expression pattern similar to AML harboring *NRAS* or *KRAS* mutations (Supplementary Fig. 6b, 6c). These results suggest that del(5q) AML may acquire RAS pathway activation through combined loss of negative regulators rather than mutational activation of a single pathway component.

We next tested whether combined inhibition of RAS negative regulators could drive AML in the absence of an activated *Ras* allele. Given the significant co-occurrence of *SPRY4*, *NF1*, and *TP53* deletions in del(5q) AML ($p < 0.0001$, Supplementary Fig. 5b), we chose to co-suppress *Spry4* and *Nf1* in a p53 null background using the HPSCs transduction/transplantation system described above. In this iteration, we knocked down *Nf1* or *Spry4* alone by introducing shRNAs coupled to mCherry (*shNf1*) or GFP (*shSpry4*) together with a control shRNA targeting Renilla Luciferase (*shRen*) of opposite color²⁵, or in combination with each other, in *Trp53*^{-/-} HPSCs (Fig. 4a for experimental design). Interestingly, suppression of *Nf1* alone led to an up-regulation of *Spry4* and vice versa (Supplementary Fig. 7a), suggesting a mutual compensatory process that accounts for the co-occurring deletions of multiple genes in this pathway. Accordingly, pErk and pS6 levels were significantly increased in premalignant *shNf1*;*shSpry4* cells compared to *shNf1*-only cells, indicating that *Spry4* contributes to a negative feedback when Ras signaling is deregulated (Supplementary Fig. 7b).

Thymectomized mice transplanted with *Trp53*^{-/-} HPSCs transduced with *Spry4* and *Nf1* shRNAs displayed accelerated leukemia onset compared with mice transplanted with any of the controls (Fig. 4b-d, Supplementary Fig. 8a). The *Trp53*^{-/-};sh*Nf1*;sh*Spry4* moribund mice presented with splenomegaly, increased white blood cell counts, and anemia (Fig. 4b), leading to a reduced overall survival (Fig. 4c, median survival of 42 days in sh*Nf1*;sh*Spry4* recipients as compared to 78 days in sh*Nf1* only recipients. $p < 0.0001$ vs. sh*Ren*, $p = 0.0027$ vs. sh*Nf1*). As expected, these *Trp53*^{-/-};sh*Nf1*;sh*Spry4* leukemia cells displayed high levels of Ras signaling (Supplementary Fig. 8b). Histopathological analyses indicated that these animals displayed leukemic blasts in the peripheral blood, their bone marrow and spleens had disrupted architecture, and leukemia cells had disseminated into the liver and other organs (Fig. 4d). Leukemic cells expressed modest levels of Gr-1, Mac-1, and Ter-119 but lacked B220 and CD3ε, as well as an increased proportion of Lin⁻;Kit⁺ myeloid progenitors consistent with an immature myeloid phenotype (Supplementary Fig. 9a, b). Leukemic cells harvested from both bone marrow and spleen produced secondary malignancies identical to the primary disease when transplanted into sub-lethally irradiated recipients, whereas *Trp53*^{-/-};sh*Nf1* disease failed to do so within the same time frame (data not shown). Thus, suppression of *Spry4* and *Nf1* cooperate in the p53 deficient background to produce AML of an early hematopoietic phenotype with myeloid maturation.

The studies above functionally validate a new tumor suppressor in del(5q) AML and in doing so provide insights into its etiology. While *CSNK1A1*, *RPS14*, *EGR1*, and *APC* have been implicated as putative tumor suppressors on this chromosome arm, the mechanism(s) by which alterations in each contribute to leukemogenesis alone or in combination is not completely understood^{26,27,28,29}. Our finding that *SPRY4* is frequently co-deleted with other negative regulators of RAS signaling suggests that one mechanism by which del(5q) can contribute to leukemogenesis is by augmenting flux through the RAS pathway. The lack of frequent mutation or silencing of the remaining allele for any gene in del(5q) deletions implies that tumor suppressors in this region are haploinsufficient^{28,29}. Accordingly, we found that the levels of *Spry4* mRNA in sh*Spry4* leukemia were halved (Supplementary Fig. 8c). These findings are consistent with the emerging view that large chromosomal deletions can contain multiple haploinsufficient tumor suppressors whose combined attenuation functionally cooperates during tumorigenesis^{30,31,32}.

In addition, our results suggest a mechanism for RAS pathway activation in del(5q) AML that may have broader significance. In contrast to other AML subtypes in which RAS signaling is activated by mutating the *NRAS*, *KRAS*, or *FLT3* oncogenes, del(5q) AMLs harbor losses of multiple RAS-signaling negative regulatory genes which can functionally cooperate to achieve high levels of RAS pathway activation. The loss of multiple negative regulators may be necessary given the typically less-potent induction of Ras-activation by negative regulator loss³³. Thus, in addition to *SPRY4* and *NF1*, *RASA1* (5q13), *DUSP1* (5q34), and *DUSP14* (17q12) are also frequently deleted in del(5q) AML and may play an important role in human disease progression. Previous work in lymphoma provides support for this model of tumor suppression, where combined haploinsufficiencies of genes in the same pathway, rather than two “hits” in a single gene, can promote tumorigenesis²⁵. Interestingly, we noted that additional cancer types with low rates of activating mutations in

the RAS pathway, such as prostate adenocarcinoma (TCGA, provisional)^{21,22} and glioblastoma³⁴, can delete multiple negative regulators that, in principle, may contribute to pathway activation in these tumor types (heterozygous/homozygous deletions of RAS negative regulators seen in 46.1% and 97.2% of cases, respectively). As such, a more thorough investigation of the functional consequences of these deletions is clearly warranted, particularly given that this could broaden patient stratification for RAS pathway targeted therapies.

Materials and methods

Retroviral constructs

LMP, LGmCreER and LMS vectors have been described previously^{1,2}. miR30-shRNAs targeting murine orthologs of the *Spry4* gene were designed using DSIR, PCR-amplified from 97-mer oligonucleotides using specific primers, digested with XhoI/EcoRI and cloned into predigested MSCV-miR30-PGK-Puromycin (LMP), MSCV-GFP-miR30-PGK-Cre (LGmCreER), or MSCV-miRe-SV40-GFP/mCherry (LMS) retroviral vectors and sequence-verified as previously described^{3,4}. LMP constructs were used for testing shSpry4 knockdown efficiency in 3T3 cells, LGmCreER constructs were used in *LSL-Kras*^{G12D}, *LSL-Kras*^{G12D};*Trp53*^{+/-} hematopoietic stem and progenitor cells (HSPCs) to introduce both self-deleting CreER and shSpry4, and LMS constructs were used in *Trp53*^{-/-} HSPCs to introduce shSpry4 and shNf1 independently. All shRNA guide sequences are listed in Supplementary Table 1.

Mouse strains

All mouse strain-related experiments were performed under the approval of the CSHL Animal Care and Use Committee and/or the MSKCC Institutional Animal Care and Use Committees. *LSL-Kras*^{G12D} and *Trp53*^{-/-} mice were backcrossed onto the C57BL/6 background for more than six generations. Genotyping was performed according to standard protocols available at <http://mouse.ncifcrf.gov>. Syngeneic C57BL/6 mice (Charles river) were used as recipients in the *LSL-Kras*^{G12D};shSpry4 HSPCs transplantation experiment shown in Supplementary Fig.2b. B6.Cg-Foxn1nu/J mice were purchased from the Jackson Laboratory (Stock number: 000819) and used as recipients in *LSL-Kras*^{G12D};*Trp53*^{+/-} HSPCs transplantation experiments shown in Fig.2, and thymectomized C57BL/6 mice were purchased from Jackson Laboratory (<http://jaxmice.jax.org/preconditioned/surgical/pricing.html>), and used as recipients in the *Trp53*^{-/-};shNf1;shSpry4 HSPCs transplantation experiments shown in Fig.4.

HSPC isolation, retroviral transduction, and transplantation

HSPC isolation and retroviral transduction were performed as described previously¹. In brief, d13.5-15.5 fetal liver cells of wildtype (WT), *LSL-Kras*^{G12D}, *Trp53*^{-/-} and *LSL-Kras*^{G12D};*Trp53*^{+/-} strain were collected. LGmCreER retroviral constructs containing GFP-coupled self-deleting CreER and the shRNAs described above were used in WT, *LSL-Kras*^{G12D}, *LSL-Kras*^{G12D};*Trp53*^{+/-} cells to introduce both Cre and the desired shRNA. To knockdown Spry4 in *LSL-Kras*^{G12D} three shRNAs targeting *Spry4* were used individually. To knockdown *Spry4* in *LSL-Kras*^{G12D};*Trp53*^{+/-} shSpry4.1865 and shSpry4.2344 were used

individually. Co-suppression of *Nf1* and *Spry4* was done by co-infecting *Trp53*^{-/-} HSPCs with miRe based MLS retroviral construct containing *shNf1*(mCherry) and three pooled shRNAs targeting *Spry4*(GFP). To induce Cre activity in vitro, infected HSPCs were treated with 0.2 μM 4-OHT (Sigma-Aldrich; dissolved in 95% cold ethanol) for 36–48 h. Approximately 2 x10⁶ cells were injected into the tail vein of 8-10-wk-old lethally irradiated syngeneic C57BL/6 mice (8.2 Gy total in single dose), 10-wk-old lethally irradiated B6.Cg-Foxn1nu/J mice (6.5 Gy total in single doses), or 10-wk-old lethally irradiated thymectomized C57BL/6 mice (7.5 Gy total in single dose) (Gammacell 40 Exactor; MDS Nordion). For secondary leukemia transplantation, ~1x10⁶ leukemia cells harvested from bone marrow or spleen were transplanted into sub-lethally irradiated syngeneic C57BL/6 recipient mice (4.5 Gy as single dose).

Quantitative RT-PCR analysis

To analyze induction of negative feedback regulators by oncogenic *Kras* expression, WT, *LSL-Kras*^{G12D} fetal liver- derived HSPCs were infected with LGmCreER without shRNA, and *Kras*^{G12D} was activated for 48 hours as described above followed by 5 days culture in the presence of cytokines as described⁵. GFP positive transduced cells were sorted before RNA extraction. Total RNA was isolated using the RNeasy Mini Kit (Qiagen) and was converted to cDNA using TaqMan Reverse Transcription Reagents (Applied Biosystems). Gene-specific primer sets were designed using Primer Express 1.5. Real-time qPCR was carried out in triplicate using SYBR Green PCR Master Mix (Applied Biosystems) on a Roche IQ5 ICycler. GAPDH or β-actin served as an endogenous control and all quantification was done using the Ct method.

For assessing in vitro target gene knockdown, *Trp53*^{-/-} HSPCs were co-infected with one of four combinations of: *shRen*;*shRen*, *shNf1*;*shRen*, *shRen*;*shSpry4* and *shNf1*;*shSpry4* (all in sequence of mCherry;GFP). Cells were grown for 4 days and then the mCherry/GFP double positive cells from all combinations were sorted for RNA isolation and RT-qPCR analysis. For *Spry4* in vivo knockdown, mCherry/GFP double positive *Trp53*^{-/-};*shNf1*;*shSpry4* leukemias were sorted and compared to mCherry positive *Trp53*^{-/-};*shNf1* leukemias that eventually grew out from the *shNf1*-mCherry;*shRen*-GFP transplant shown in Fig. 4). qPCR primers are listed in Supplementary Table 2.

Histocytological and molecular characterization of myeloid malignancy

Peripheral blood was obtained from recipient mice during leukemogenesis and at terminal disease stage and blood smears were stained with Wright-Giemsa stain. Animals were sacrificed by CO₂ euthanasia upon severe leukocytosis, enlarged spleen and/or moribund appearance. Organs were fixed in 10% neutral buffered formalin and were processed to obtain paraffin sections for histological staining. Bone marrow cells were flushed from tibias and femurs and spleens were homogenized in IMDM containing 1% BSA. Erythrocytes were then lysed in ACK (150 mM NH₄Cl, 10 mM KHCO₃, 0.1 mM EDTA) for 5 min, and nucleated cells were resuspended in IMDM/1% BSA and filtered through a nylon screen (100 μm) to obtain single-cell suspensions. PCR analysis of Cre-mediated recombination was as described¹ and *Trp53* LOH analysis was done using *Trp53* genotyping primers as described by Jackson Laboratory. . *Trp53* exon-sequencing primers are available from the

authors upon request. Whole bone marrow and spleen cells were stained with antibodies for Sca-1, Kit, Mac-1, Gr-1, B220, Thy1, CD3 ϵ , CD4, CD8 and Ter-119 (BD Biosciences and eBioscience). Flow cytometry was run on an LSR-II or Fortessa flow cytometer (BD Biosciences), and analyzed using FACSDiva (BD Biosciences) and FlowJo (Treestar) software.

Phospho-FACS

These procedures were carried out as described previously^{1,6}. GM-CSF was used as stimulation cytokine in initial *Kras*^{G12D};*shp53* AML model due to the mature myeloid nature of the leukemia. In *Trp53*^{+/-};*Kras*^{G12D};*shSpry4* experiment, serum was used as a broad extrinsic activation mechanism for Ras signaling pathway for sarcoma cells with or without the myeloid marker Mac-1. Due to the relative immature phenotype of *Trp53*^{-/-};*shNf1*;*shSpry4*, IL-3 was used as it activates a broader range of cells including myeloid progenitors and mature myeloid cells. To quantify signaling intensity, relative MFI was defined as (MFI of GFP+ cells)/(MFI of GFP-cells) (Fig.1b, Supplementary Fig.1a-d), and as (MFI with primary antibody)/(MFI without primary antibody) in cases of dual fluorescence markers (mCherry and GFP) used (Supplementary Fig.7b).

Immunoblotting analysis

For *Kras* expression comparison, GFP positive *Kras*^{G12D} only and *Kras*^{G12D};*shp53* leukemic cells were sorted and lysed in Laemmli buffer. Equal amounts of protein were separated on 12% SDS–polyacrylamide gels and transferred to PVDF membranes. *Kras* antibody (F234, sc-30) was used for detecting level of total *Kras* and the abundance of β -actin was monitored to ensure equal loading. Images were analyzed using the AlphaView software (ProteinSimple). For *Spry4* knockdown analysis, NIH 3T3 cells were first infected with an MSCV-5xFlag-*Spry4*-hygro construct and selected with hygromycin to generate a stable line expressing Flag-*Spry4*. These cells were then infected with MLP-based *shSpry4* once for low MOI and three times for high MOI. After selection with puromycin, cells were lysed for protein extraction as described⁷. The F1804 monoclonal anti-flag M2 antibody (Sigma) was used for detecting expression of *Spry4*.

Genomic data analysis

Copy number aberrations and chromosome deletions were based on available TCGA Acute Myeloid Leukemia data⁸. Raw data was downloaded from TCGA Data Portal. Cancer genome datasets and bioinformatics tools for visualizing different parameters for analysis of genomic data are accessible through MSKCC cBioPortal (www.cbioportal.org). Copy number states (homozygous deletion, hemizygous deletion, gain, and amplification) were determined from Affymetrix SNP 6.0 platform by the copy number analysis algorithms GISTIC (PMID:21527027) and RAE (PMID: 18784837).

Human AML samples were obtained from the University of Chicago. SNP array based copy number analyses of 35 samples are from published results⁹, and data analysis and expression level estimates were performed as described⁹. Gene set enrichment analysis was performed using the GSEA method GSEA v2.1.0 (Gene set enrichment analysis—Broad Institute)

(PMID: 16199517). Multiple testing adjusted p-value (FDR.q.val) less than 0.05 were considered statistically significant.

Statistics and general methods

For animal survival studies, at least 5 mice per experimental category were used, while for biochemical studies, 3 mice per group were utilized. Significant results were subsequently confirmed in independent experiments and presented in all figures as biological replicates. Animals were housed and used randomly, and the investigators were not blinded to the experiments, with the exception of histopathological analysis. No exclusion of data was carried out, except in cases of overall survival curves, when mice were censored if premature death was caused by non-biological factors (i.e. animals euthanized for a pre-disease endpoint).

Differences between groups were calculated using *t*-test or ANOVA, or with Welch's correction when variance was not similar between groups. Murine gene suppression was analyzed by Column Statistics. For animal transplantation experiments, statistical evaluation of overall survival was based on the log-rank (Mantel-Cox) test for comparison of the Kaplan- Meier event time format. Co-occurrence analyses were derived from the MSKCC cBioPortal or by Fisher's exact test and a permutation test comparing the observed number of co-occurrent events with the expected number of co-occurrent events under a null distribution generated by 10,000 sample permutation (pre-existing).

Supplementary Material

Refer to Web version on PubMed Central for supplementary material.

Acknowledgements

The authors gratefully acknowledge Agustin Chicas, Ozlem Aksoy, Chun-Hao Huang and Chong Chen for their expert technical assistance, advice, and supportive data, as well as members of the Lowe laboratory for helpful comments. The authors also thank Charles Sherr and Shane Mayack for editorial comments on the manuscript. This study was supported by a Specialized Center of Research (SCOR) grant from the LLS, a Starr Cancer Consortium Grant, the Don Monti Memorial Research Foundation, the Geoffrey Beene Center for Cancer Research, a Award from Ministry of Education of Taiwan to C.C. and a LLS Research Fellow Award to C.D.R. (5428-15). S.W.L. is an Investigator in the Howard Hughes Medical Institute.

References

1. Genomic and epigenomic landscapes of adult de novo acute myeloid leukemia. *N Engl J Med.* 2013; 368:2059–2074. [PubMed: 23634996]
2. Bullinger L, et al. Use of gene-expression profiling to identify prognostic subclasses in adult acute myeloid leukemia. *N Engl J Med.* 2004; 350:1605–1616. [PubMed: 15084693]
3. Patel JP, et al. Prognostic relevance of integrated genetic profiling in acute myeloid leukemia. *N Engl J Med.* 2012; 366:1079–1089. [PubMed: 22417203]
4. Schubbert S, Shannon K, Bollag G. Hyperactive Ras in developmental disorders and cancer. *Nat Rev Cancer.* 2007; 7:295–308. [PubMed: 17384584]
5. Feldser DM, et al. Stage-specific sensitivity to p53 restoration during lung cancer progression. *Nature.* 2010; 468:572–575. [PubMed: 21107428]
6. Junttila MR, et al. Selective activation of p53-mediated tumour suppression in high-grade tumours. *Nature.* 2010; 468:567–571. [PubMed: 21107427]

7. Xu J, et al. Dominant role of oncogene dosage and absence of tumor suppressor activity in Nras-driven hematopoietic transformation. *Cancer Discov.* 2013; 3:993–1001. [PubMed: 23733505]
8. Zhao Z, et al. p53 loss promotes acute myeloid leukemia by enabling aberrant self-renewal. *Genes Dev.* 2010; 24:1389–1402. [PubMed: 20595231]
9. Braun BS, et al. Somatic activation of oncogenic Kras in hematopoietic cells initiates a rapidly fatal myeloproliferative disorder. *Proc Natl Acad Sci U S A.* 2004; 101:597–602. [PubMed: 14699048]
10. Van Meter ME, et al. K-RasG12D expression induces hyperproliferation and aberrant signaling in primary hematopoietic stem/progenitor cells. *Blood.* 2007; 109:3945–3952. [PubMed: 17192389]
11. Courtois-Cox S, et al. A negative feedback signaling network underlies oncogene-induced senescence. *Cancer Cell.* 2006; 10:459–472. [PubMed: 17157787]
12. Xue W, et al. Senescence and tumour clearance is triggered by p53 restoration in murine liver carcinomas. *Nature.* 2007; 445:656–660. [PubMed: 17251933]
13. Chicas A, et al. Dissecting the unique role of the retinoblastoma tumor suppressor during cellular senescence. *Cancer Cell.* 2010; 17:376–387. [PubMed: 20385362]
14. Kim HJ, Bar-Sagi D. Modulation of signalling by Sprouty: a developing story. *Nat Rev Mol Cell Biol.* 2004; 5:441–450. [PubMed: 15173823]
15. Chen C, et al. MLL3 is a haploinsufficient 7q tumor suppressor in acute myeloid leukemia. *Cancer Cell.* 2014; 25:652–665. [PubMed: 24794707]
16. Zhang J, et al. Oncogenic Kras-induced leukemogenesis: hematopoietic stem cells as the initial target and lineage-specific progenitors as the potential targets for final leukemic transformation. *Blood.* 2009; 113:1304–1314. [PubMed: 19066392]
17. Sabnis AJ, et al. Oncogenic Kras initiates leukemia in hematopoietic stem cells. *PLoS Biol.* 2009; 7:e59. [PubMed: 19296721]
18. Douet-Guilbert N, et al. Molecular characterization of deletions of the long arm of chromosome 5 (del(5q)) in 94 MDS/AML patients. *Leukemia.* 2012; 26:1695–1697. [PubMed: 22290067]
19. Zhao N, et al. Molecular delineation of the smallest commonly deleted region of chromosome 5 in malignant myeloid diseases to 1-1.5 Mb and preparation of a PAC-based physical map. *Proc Natl Acad Sci U S A.* 1997; 94:6948–6953. [PubMed: 9192672]
20. Jerez A, et al. Topography, clinical, and genomic correlates of 5q myeloid malignancies revisited. *J Clin Oncol.* 2012; 30:1343–1349. [PubMed: 22370328]
21. Cerami E, et al. The cBio cancer genomics portal: an open platform for exploring multidimensional cancer genomics data. *Cancer Discov.* 2012; 2:401–404. [PubMed: 22588877]
22. Gao J, et al. Integrative analysis of complex cancer genomics and clinical profiles using the cBioPortal. *Sci Signal.* 2013; 6:p11. [PubMed: 23550210]
23. Bowen DT, et al. RAS mutation in acute myeloid leukemia is associated with distinct cytogenetic subgroups but does not influence outcome in patients younger than 60 years. *Blood.* 2005; 106:2113–2119. [PubMed: 15951308]
24. Kadia TM, et al. Clinical and proteomic characterization of acute myeloid leukemia with mutated RAS. *Cancer.* 2012; 118:5550–5559. [PubMed: 22569880]
25. Scuoppo C, et al. A tumour suppressor network relying on the polyamine-hypusine axis. *Nature.* 2012; 487:244–248. [PubMed: 22722845]
26. Schneider RK, et al. Role of Casein Kinase 1A1 in the Biology and Targeted Therapy of del(5q) MDS. *Cancer Cell.* 2014; 26:509–520. [PubMed: 25242043]
27. Ebert BL, et al. Identification of RPS14 as a 5q- syndrome gene by RNA interference screen. *Nature.* 2008; 451:335–339. [PubMed: 18202658]
28. Joslin JM, et al. Haploinsufficiency of EGR1, a candidate gene in the del(5q), leads to the development of myeloid disorders. *Blood.* 2007; 110:719–726. [PubMed: 17420284]
29. Wang J, Fernald AA, Anastasi J, Le Beau MM, Qian Z. Haploinsufficiency of Apc leads to ineffective hematopoiesis. *Blood.* 2010; 115:3481–3488. [PubMed: 20065296]
30. Xue W, et al. A cluster of cooperating tumor-suppressor gene candidates in chromosomal deletions. *Proc Natl Acad Sci U S A.* 2012; 109:8212–8217. [PubMed: 22566646]
31. Davoli T, et al. Cumulative haploinsufficiency and triplosensitivity drive aneuploidy patterns and shape the cancer genome. *Cell.* 2013; 155:948–962. [PubMed: 24183448]

32. Solimini NL, et al. Recurrent hemizygous deletions in cancers may optimize proliferative potential. *Science*. 2012; 337:104–109. [PubMed: 22628553]
33. Cutts BA, et al. Nf1 deficiency cooperates with oncogenic K-RAS to induce acute myeloid leukemia in mice. *Blood*. 2009; 114:3629–3632. [PubMed: 19710506]
34. Brennan CW, et al. The somatic genomic landscape of glioblastoma. *Cell*. 2013; 155:462–477. [PubMed: 24120142]

References for Methods

1. Zhao Z, et al. p53 loss promotes acute myeloid leukemia by enabling aberrant self-renewal. *Genes Dev*. 2010; 24:1389–1402. [PubMed: 20595231]
2. Dickins RA, et al. Probing tumor phenotypes using stable and regulated synthetic microRNA precursors. *Nat Genet*. 2005; 37:1289–1295. [PubMed: 16200064]
3. Dow LE, et al. A pipeline for the generation of shRNA transgenic mice. *Nat Protoc*. 2012; 7:374–393. [PubMed: 22301776]
4. Fellmann C, et al. An Optimized microRNA Backbone for Effective Single-Copy RNAi. *Cell Rep*. 2013; 5:1704–1713. [PubMed: 24332856]
5. Schmitt CA, et al. Dissecting p53 tumor suppressor functions in vivo. *Cancer Cell*. 2002; 1:289–298. [PubMed: 12086865]
6. Van Meter ME, et al. K-RasG12D expression induces hyperproliferation and aberrant signaling in primary hematopoietic stem/progenitor cells. *Blood*. 2007; 109:3945–3952. [PubMed: 17192389]
7. Hemann MT, et al. An epi-allelic series of p53 hypomorphs created by stable RNAi produces distinct tumor phenotypes in vivo. *Nat Genet*. 2003; 33:396–400. [PubMed: 12567186]
8. Genomic and epigenomic landscapes of adult de novo acute myeloid leukemia. *N Engl J Med*. 2013; 368:2059–2074. [PubMed: 23634996]
9. McNerney ME, et al. CUX1 is a haploinsufficient tumor suppressor gene on chromosome 7 frequently inactivated in acute myeloid leukemia. *Blood*. 2013; 121:975–983. [PubMed: 23212519]

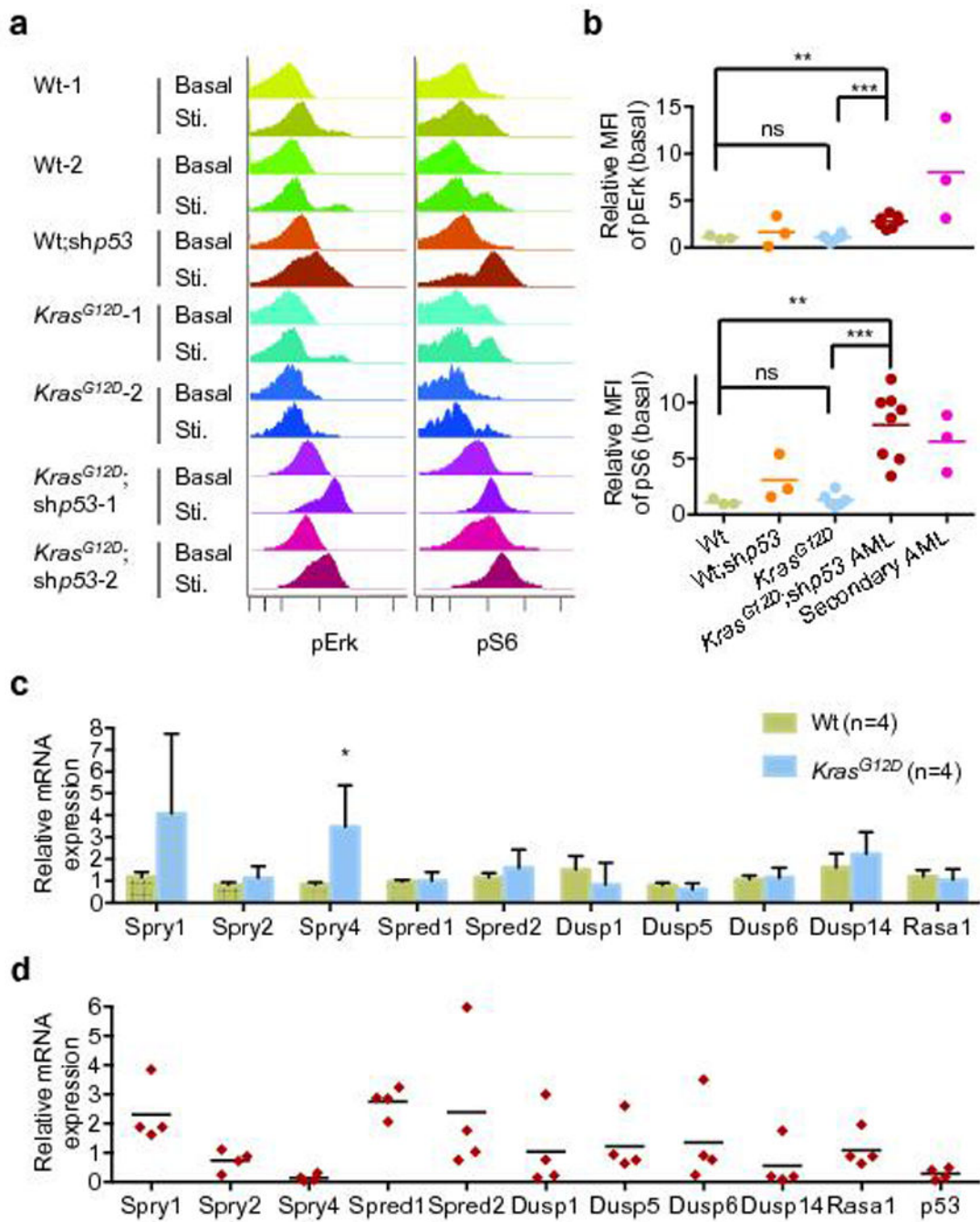


Fig. 1. Reduced *Spry4* expression correlates with increases in Ras-signaling during *Kras*^{G12D} induced leukemogenesis

a. Representative phospho-signaling analysis (phospho-FACS) showing basal and cytokine-responsive (GM-CSF stimulation) pErk and pS6 levels are enhanced in *Kras*^{G12D};shp53 leukemia relative to non-leukemic bone marrow (BM) cells derived from WT, WT;shp53 or *Kras*^{G12D} (*Kras*-1, *Kras*-2) mice.

b. Quantification of basal pErk (top) and pS6 (bottom) levels showing significant elevation of signaling in primary and secondary leukemia. Relative Mean Fluorescence Intensity

(MFI) was calculated by dividing MFI of GFP⁺ (LGmCreER) infected cells with MFI of GFP⁻ uninfected cells from the same animal. Data was derived from primary recipient mice transplanted with independently generated and infected HSPCs (n = 3–8 each group. * $p < 0.05$, ** $p < 0.01$, *** $p < 0.001$. Two tailed t- test, with Welch's correction when applicable).

c. RT-qPCR analyses showing significant induction of *Spry4* upon *Kras*^{G12D} activation in HSPCs. Data was derived from two experiments using independently generated and infected HSPCs (n = 4, * $p < 0.05$. Two-way repeated measures ANOVA, bar graph shown as mean \pm SD).

d. RT-qPCR analyses showing RNA expression of the same genes as in (c) in *Kras*^{G12D};shp53 leukemia cells relative to normal BM (normalized to 1 for all genes). Note the suppression of *Trp53* and *Spry4* in all independently derived primary samples (n = 4, Column Statistics).

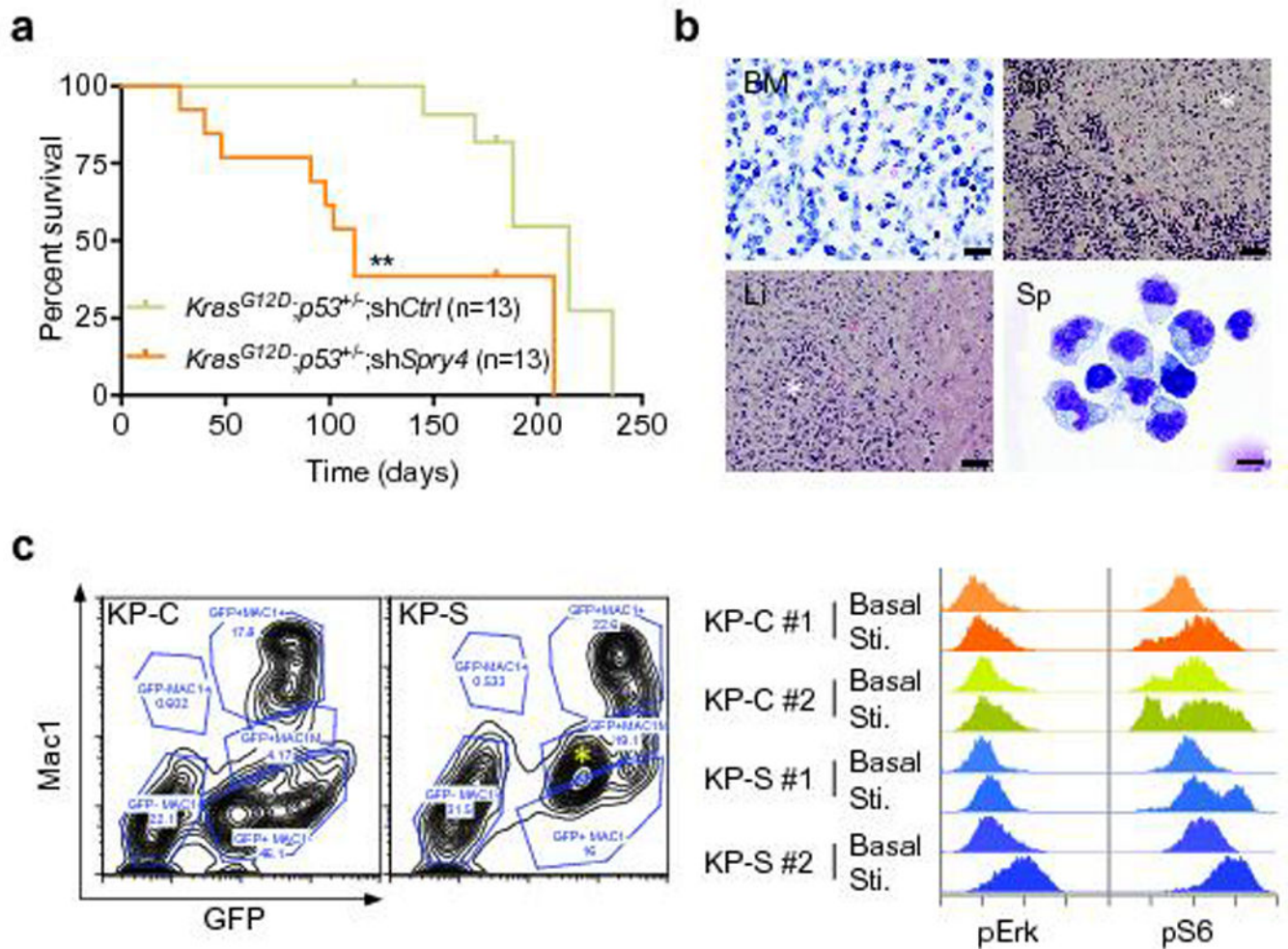


Fig. 2. Spry4 knockdown accelerates leukemogenesis

a. Kaplan-Meier curve of overall survival of mice reconstituted with $Kras^{G12D};Trp53^{+/-};shSpry4$ HSPCs (KP-S) in comparison with control shRNA recipients (KP-C). Data was derived from two independent experiments using independently generated and infected HSPCs (** $p < 0.01$).

b. Representative histopathology of $Kras^{G12D};Trp53^{+/-};shSpry4$ histiocytic sarcomas: malignant cells are present in the bone marrow (BM), liver (Li) and spleen (Sp) (* indicates histiocytes in images of liver and spleen), as shown by hematoxylin and eosin staining. Spleen includes numerous cells with a monocytic to histiocytic appearance by cytospin and Wright-Giemsa staining (bottom right panel). Size bar represents 12 microns for BM (100x), 30 microns for liver and spleen (40x), and 8 microns for cytospin (100x).

c. (Left) Flow cytometry analyses showing expansion of Mac-1 intermediate population (GFP⁺Mac1^M) in spleen of $Kras^{G12D};Trp53^{+/-};shSpry4$ (KP-S) recipients (population marked with *). Also shown is gating strategies based on level of Mac-1 expression (GFP⁺Mac-1⁺, GFP⁺Mac-1^M and GFP⁺Mac-1⁻).

d. (Right) Representative phospho-FACS analyses showing basal and serum-responsive (Sti) pErk and pS6 levels of malignant histiocytic sarcoma cells derived from

Kras^{G12D};*Trp53*^{+/-};sh*Spry4* (KP-S) and in *Kras*^{G12D};*Trp53*^{+/-};sh*Ctrl* (KP-C) animals. KP-S recipients show enhanced responsive pErk and pS6 levels in GFP⁺Mac1^M population when compared with the same cell population in *Kras*^{G12D};*Trp53*^{+/-};sh*Ctrl* (KP-C) animals. Data was derived from independent primary histiocytic sarcomas induced by independently generated and infected HSPCs (n = 2–3 each group).

Author Manuscript

Author Manuscript

Author Manuscript

Author Manuscript

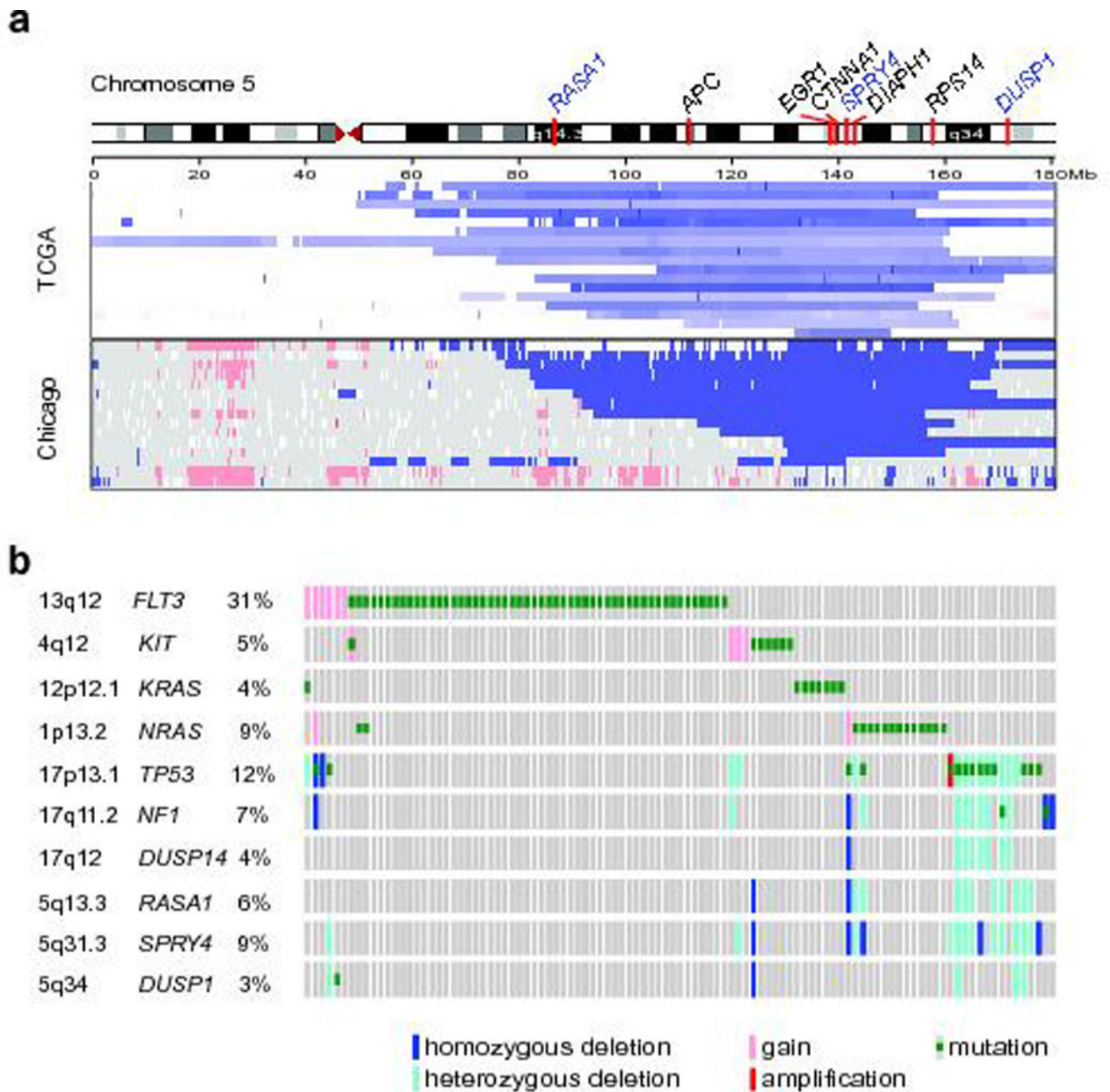


Fig. 3. *SPRY4* and other negative regulators of the RAS pathway are deleted in del(5q) AML
 a. (Top Panel) Chromosome 5 copy number analysis of AML patients published within the AML TCGA dataset. Deletions (purple) involving various regions of chromosome 5q include *SPRY4* in 17 samples. (Bottom Panel) In a set of 35 patients (Chicago dataset) with de novo AML or t-MNs analyzed by SNP array, 13 samples exhibit deletion of *SPRY4* (among 15 samples shown 13 samples have $-5/\text{del}(5q)$ detected by cytogenetic analysis, of which 12 show *SPRY4* deletions; 1 additional *SPRY4*-deleted sample without cytogenetic information).

b. Putative copy number alterations in the TCGA dataset showing deletion of negative feedback regulatory genes on 5q and 17q, in the context of mutation and/or deletion of *TP53*. Notably, these lack mutation and/or amplification in *FLT3*, *KIT*, and *RAS*. The genomic location and alteration frequency of all genes is shown on the left. For clarity, only the 103 cases that have the above alterations (total 187 cases) are shown (cBioPortal link in M&M section).

Author Manuscript

Author Manuscript

Author Manuscript

Author Manuscript

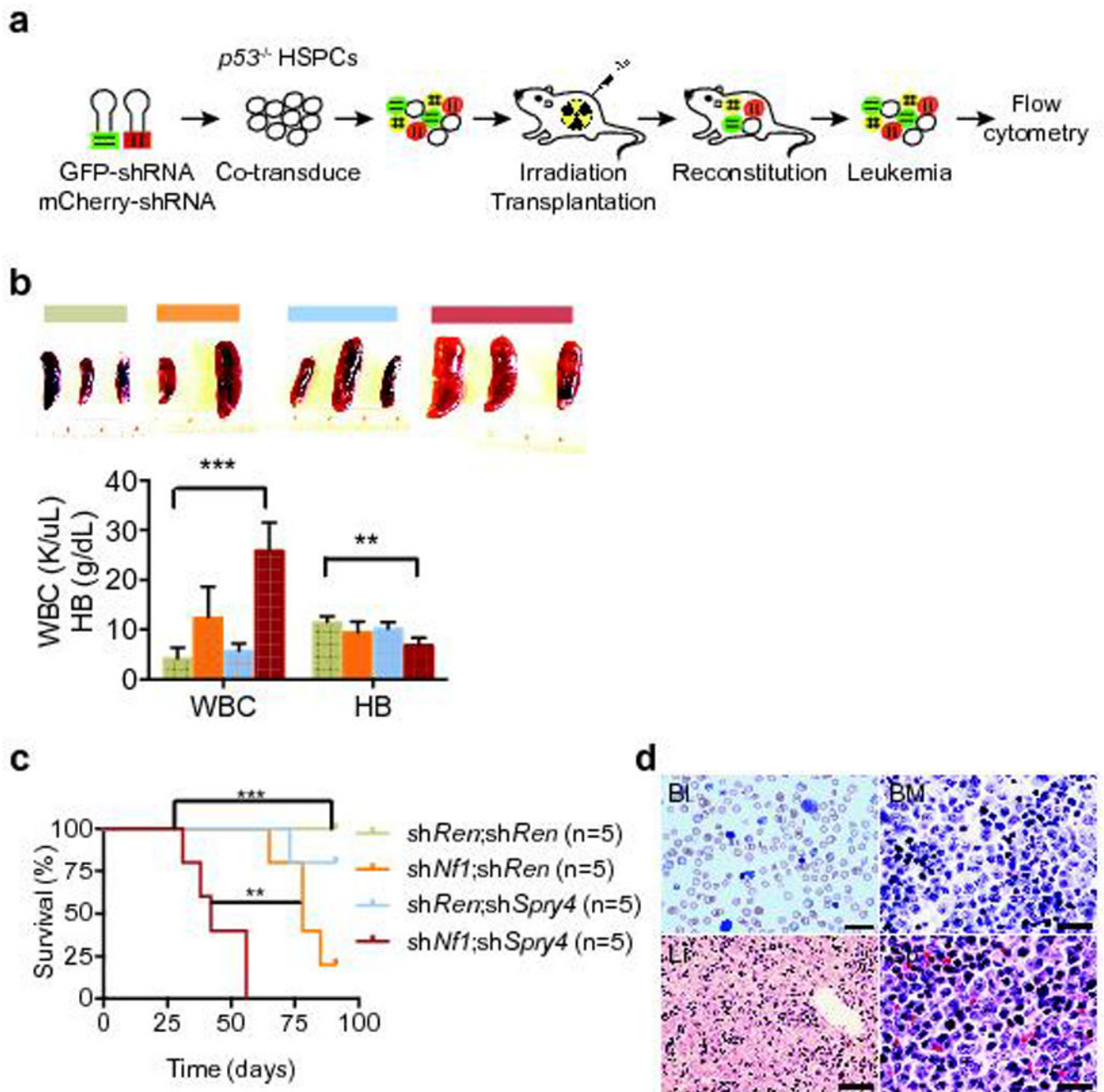


Fig. 4. Suppression of Nf1 and Spry4 cooperate to promote myeloid leukemogenesis

a. Schematic showing experimental design to test the cooperation between suppression of Nf1 and Spry4 in the background of Trp53 deficiency. Combinations tested were *shRen;shRen*, *shNf1;shRen*, *shRen;shSpry4* and *shNf1;shSpry4* (mCherry;GFP).

b. Splenomegaly was consistently found in mice reconstituted with *Trp53*^{-/-}; *shNf1;shSpry4* HSPCs after 5 weeks. Peripheral blood analyses of *Trp53*^{-/-}; *shNf1;shSpry4* recipient mice at 8-weeks shows elevated WBC count (in K/ μ L) and reduced level of hemoglobin (in g/dL) (n = 2–5 in each group. ***p* < 0.01, *** *p* < 0.0001. Two tailed *t*-test, bar graph shown as mean \pm SD).

c. Kaplan-Meier curve showing that mice reconstituted with *Trp53*^{-/-};*shNf1*;*shSpry4* HSPCs have a significantly reduced overall survival (n = 5 in all groups. ***p* < 0.01, *** *p* < 0.0001).

Histopathology analysis showing leukemia in peripheral blood (Bl), bone marrow (BM), liver (Li) and spleen (Sp) by hematoxylin and eosin staining. Size bar represents 20 microns for BM and spleen (100x), 50 microns for liver (40x), and 33 microns for blood (60x).